Guide to NSTX GPI data

S.J. Zweben and R.J. Maqueda,
A. Diallo, F. Scotti, D. Stotler, T. Stoltfus-Dueck et al

DRAFT v.4
5/10/18

OUTLINE

1. GPI collaborators on NSTX
2. GPI hardware information
3. Overview of 2010 GPI data
4. Viewing and restoring GPI data
5. Data analysis issues for GPI
6. Possible GPI upgrades for NSTX-U
7. Further GPI analysis with existing data
8. Future experiments on NSTX-U
9. Possible collaborations
10. List of publications

1. GPI collaborators on NSTX

Daren Stotler, Bill Davis, Ahmed Diallo, Noah Mandell, Tim Stoltzfus-Dueck – PPPL
Jim Myra, Dan D'Ippolito and David Russell – Lodestar
Yancy Sechrest and Tobin Munsat – Colorado
Matteo Agostini and Paolo Scarin – RFX group Padova
Filippo Scotti – LLNL
Santanu Banerjee - IPP (India)
K.F. Gan (U. Tennessee)
Bin Cao – Hefei (China)
John Lowrance, Vince Mastrocola, George Renda – Princeton Scientific Instruments
Jim Terry MIT
Anne White – UCLA/MIT
Arturo Alonso – CIEMAT (Spain)
Nobu Nishino – Hiroshima (Japan)
Glen Wurden - LANL

2. Hardware information

2.1 NSTX GPI hardware history

2000 - first view of gas puffs with LANL Kodak camera
2002 - re-entrant GPI port at Bay B installed

2002 - Phantom 4 at slow speed
2003 - PSI-4 camera (28 frames)
2004 - PSI-5 camera (300 frames)
2005 - photomultiplier array added
2007 - Phantom 7.1 and 7.3
2009 - Phantom 710
2015 - new bundle, zoom lenses

All existing ex-vessel GPI hardware is presently in 020A, including:

- Phantom 710 camera used for GPI (P28651, owned by B. Stratton SN9205)
- Dell computer used to run GPI from control room (M46057, owned by Brent)
- new zoom GPI optics and new coherent fiber bundle on 2'x3' optical bench
- old GPI optics and old (browned) coherent fiber bundle in a box
- large 68 mm GPI Dalpha (656 nm) filter screwed onto Phantom camera lens
- GPI target/calibration plate which attaches to GPI manifold inside vessel
- some older filters were given to Filippo for safekeeping

2.2 In-vessel hardware

Since ~2002 the GPI in-vessel hardware has been essentially the same, as shown in Fig. 1 (taken in 2014). The GPI re-entrant viewing port is located just below the outer midplane in Bay B, and the GPI gas manifold is located just above the midplane next to the (original) NBI port. The manifold was moved a couple of cm closer to the plasma and downward from 42º to 36º for the 2004 run, but has been at the same location since then.

The re-entrant viewport is tilted upward from the horizontal so that the optics inside it can view the gas from the manifold approximately along the local B field line. The gas manifold is designed to form a gas cloud matching the GPI field of view in the poloidal (i.e. bi-normal) direction, with 30 holes of 1 mm diameter, 1 cm apart facing inward toward the plasma (top right of Fig. 1). The viewport is a quartz window which is covered by a radial shutter between shots (lower right of Fig. 1). Original drawings for the re-entrant port and manifold are in the NSTX GPI Guide folder ("GPI Drawings"). Both the window and the manifold holes get coated over time and are cleaned during openings.

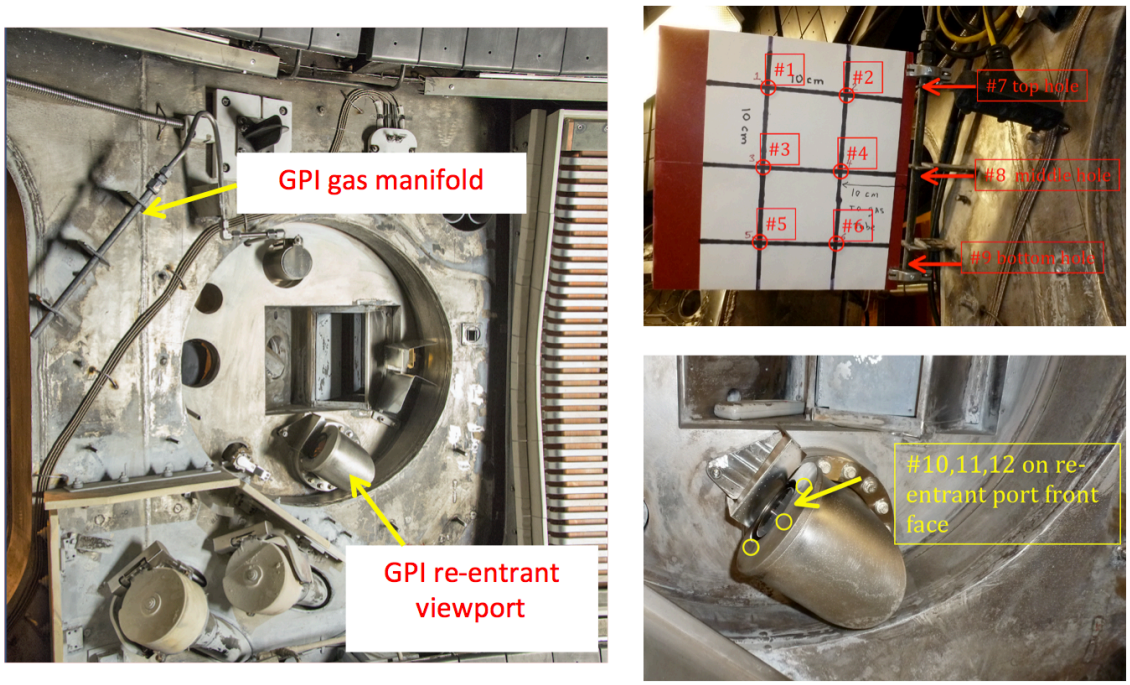

Fig. 1 – GPI in-vessel hardware (2014)

2.3 Gas puff hardware

The gas puff hardware for 2002-2014 consisted of a piezoelectric valve (PV-40) and a small gas reservoir plenum (26.82 cm^3) located just outside Bay B ("Bay B high-flow"). The gas could be switched to either D_2 or He before a run day. The plenum pressure, puff trigger time, and puff duration were set by a machine operator before each shot (and could be repeated automatically on successive shots). For this period there was only one puff per shot, usually done during the steady-state part of the shot.

The gas puff hardware was not changed significantly from 2002-2014. The gas puff parameters for shots in this period (at least for the 2010 run) can be found by running /p/gpi/szweben/gas_3.pro. Typical plenum pressures were 1.5-2 bar and piezo opening durations usually 20-30 msec. The total gas puff into the vessel was calculated from the measured pressure drop and plenum volume, typically ~5 Torr-liters. It was checked once or twice by closing off all the vessel pumping and measuring the pressure rise in the chamber (Bill Blanchard estimated the uncertainty as ±10%). More information about the gas puff is in a memo "GasNodeSummary" by Paul Sichta in the GPI Guide Equipment folder, and in the paper Zweben et al, PPCF 56, 095010 (2014).

The GPI gas puff was disconnected during the long outage ~2012, and a new gas control system for NSTX-U was implemented for the 2016 run. This new system was capable of turning the puff on/off more than once a shot, so would have been useful. However, the GPI gas lines were not re-connected before the end of the short run in 2016, so the last GPI data was in the 2010 run.

2.4 In-vessel calibration

The spatial location of the in-vessel GPI hardware components was measured during most machine openings using the standard measuring arm. The procedure for the 2014 and 2016 calibrations is in the Guide notes in the folder "GPI calibration", along with the calibration results (Excel files). The location of the manifold and re-entrant port did not vary from year-to-year, but the "target plate" for alignment of the GPI field of view was reinstalled on the manifold every year, and its design was varied slightly over the years. The target plate and measuring locations for 2014 were shown in Fig. 1.

A summary of the resulting GPI geometry is summarized in Table 1, taken from Zweben et al, Phys. Plasmas 24, 102509 (2017). Here the "optical vertex" is the approximate location of the focal point of the front-end lens (after correcting for the reflection from the front-end mirror), and the image center is the central point of the camera image at pixel (32,40) for the 2010 run. As of 4/18, Filippo found that the vertex location in this table was not quite correct since the resulting view to the GPI optics does not go through the window (this does not significantly affect the target plate calibration results). Filippo suggests future calibrations be done using two toroidal planes, not just one

Table 1 – GPI geometry in NSTX

	R (cm)	z (cm)	Toroidal angle (deg)
Optical vertex @ lens	170.2	−21.4	43
Image center @ (32,40)	149.1	19.9	62
Distance from the optical vertex to the image center = 69 cm			
Vertical angle of the GPI view @ the image center (32,40) = 36.8°			

2.5 Optics

The front-end optics inside the re-entrant port was essentially the same since ~2002-2010, as shown in Fig. 2. It consists of an oval front-surface mirror and a fixed mount for a commercial lens. The lens is coupled to a glass Schott IG-163 coherent fiber optic bundle of length ~4.5 m with 800x1000 fibers (see "Schott specs" in "GPI equipment" folder in the GPI Guide). The front end optics was bolted into a port at Bay B with the view aligned to see through the re-entrant port window (this optics was sometimes removed from the port for calibrations). This attachment was unchanged from 2002-2010. The bundle gradually browned due to radiation over the years, and by the end of 2010 had a transmission of only ~8% in the red (compared with ~25% when new). The front-end optics and bundle were significantly changed for the 2016 run, as described in the folder "GPI zoom optics" in the GPI guide.

Fig. 2 - original front-end GPI optics (left) and 2018 GPI optical bench (right)

The other end of the bundle was mounted on a 2'x3' optical bench in a stand located just outside Bay B (see Fig. 2). The light from the bundle was focused at infinity by the lens at the back end of the bundle, then passed through an interference filter to isolate either Dα (656 nm) or HeI (587.6 nm) lines. The image was then de-magnified by another lens on the camera to form an image on the sensor typically 64x80 pixels (for the 2010 run).

Prior to the 2010 run the image was sometimes split by a beam-splitter on the optical bench to send some fraction of the light to a second camera (2009) or to the photomultiplier array (~2005-2008). This was not done in 2010 for the Phantom 710 data, which used all the light to make good images at 400,000 frames/sec.

2.6 Detectors and absolute calibration

As noted in Sec. 2.1, several different detectors were used for GPI in NSTX. The most extensive set of data was taken for the 2010 run with the Phantom 710 camera, normally with 64x80 pixels at just under 400,000 frames/sec. Good data was also taken for the 2009 run with an interleaved combination of a Phantom 7.1 and 7.3 cameras. Earlier data with the PSI cameras is probably not useful at this stage. The photomultiplier array used ~2005-2008 was used for getting high speed data and long time coverage before the Phantom cameras, but is probably not useful at this stage.

Normally the absolute amount of the light emission is not important in analyzing the edge turbulence, as long as the signal level is high enough. However, there was a special effort by a visiting Chinese student Bin Cao in 2011 in collaboration with Daren to do an absolute calibration of the 2010 GPI optics for the purpose of validating the DEGAS 2 neutral code. The results of this work were published as B. Cao et al, Fusion Science and Technology 64, 29 (2013). The amount of light per injected D_2 atom was

within about ~40% of the amount predicted by DEGAS 2 modeling, which was about as good as could be expected given the many sources of uncertainty.

2.7 Camera stand and shielding

For 2002-2014 the optical bench for the GPI was mounted in a stand just outside Bay B. Since this blocked the vessel entry at Bay A, the stand had to be removed during machine openings and replaced before each run. This also made the in-vessel optical calibrations for GPI more difficult since the camera was not in its normal place during the calibration. Plans were being made to move the stand after the 2016 run, along with the installation of the APD array (see folder "GPI future plans/APD installation by MIT").

At some point ~2004 we installed substantial lead and borated polyethylene shielding around the PSI-4 and/or PSI-5 cameras next to Bay B, since we were seeing neutron/gamma noise in the images from the plasma in the cameras. This was not needed for the Phantom cameras so was not used for the 2009-2010 runs. The lead had to be supported by a vertical column in the basement, which was removed during the long outage ~2014. The PM tubes were mounted in a separate shielded igloo near the wall of the test cell at Bay B.

Filippo may add something about the networking interface here.

2.8 Reinstalling GPI on NSTX-U

This is what needs to be done to get existing GPI hardware working on NSTX-U:

- GPI gas line needs to be reconnected (was taken off for Upgrade ca. 2013)
- determine if lead shielding for camera/bundle is needed for higher neutron rate
- determine if magnetic shielding is needed for camera due to higher fields
- identify better mounting location for GPI camera outside Bay B midplane
- design and install new camera stand and its physical/electrical support
- test LabView camera control software on PC and upgrade if necessary
- review choice of camera and front-end lenses to define imaging field of view
- clean holes in GPI gas manifold and check gas fittings inside vessel
- test camera operation with computer (may need new camera trigger cable)
- test new gas puff control system without vacuum, to whatever extent possible
- install re-entrant optics on Bay B midplane port and remote camera controls
- do in-vessel calibration with target plate (preferably w/ final camera location)
- absolutely calibrate GPI gas puffer in Torr-liters with D_2 and He (into vacuum)
- test camera triggering and data transfer/storage from GPI PC to main computers

Some of the existing GPI installation procedures are in folder "GPI installations" in the GPI calibrations folder in the Guide. All the official GPI procedures are also in the NSTX operation documents archive.

3. Overview of 2010 GPI data

There is a large set of good GPI data taken with the Phantom 710 camera for the 2010 run which can be used for further analysis, even though this data has already been the subject of several previous papers from 2013-2017 (see list in Sec. 10). The location of the GPI view for 2010 is illustrated in Fig. 3, taken from Zweben et al PPCF 56, 095101 (2014).

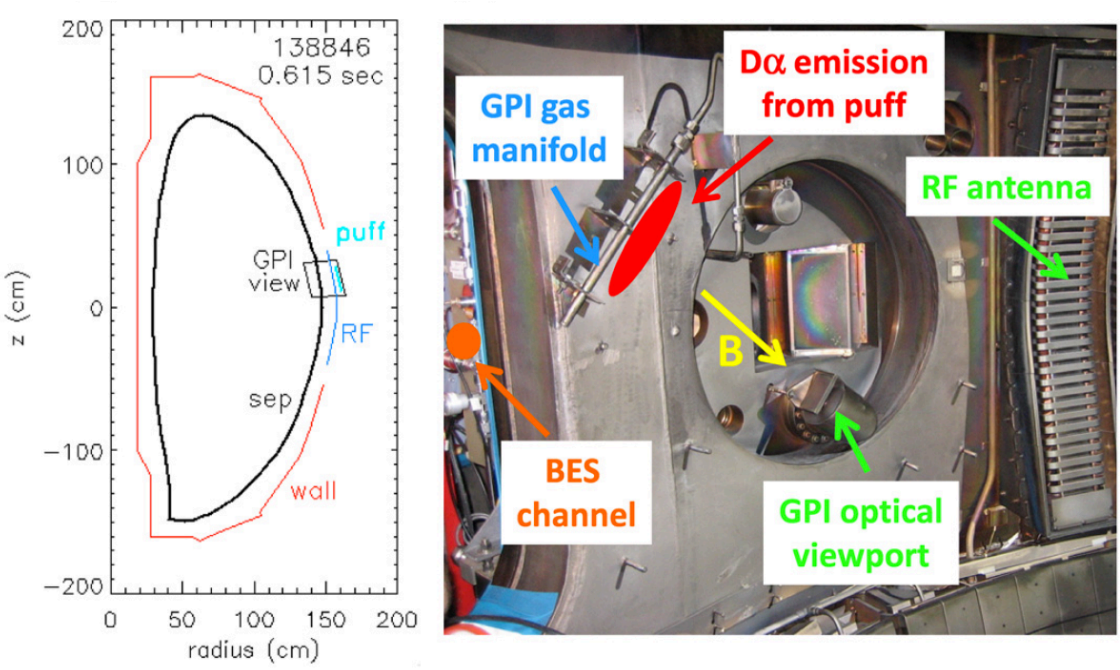

Fig. 3 - GPI view in machine for 2010 run

An annotated Excel shot list of 322 shots taken at the fastest frame rate of ~400,000 frames/sec covering #137585-142275 was made by Ricky, and is in the GPI Guide ("GPI shot lists" folder in the Guide). These shots are from many different XPs and so do not represent a single systematic scan, but do cover almost the entire parameter range of NSTX operation. Subsets of this data which have already been analyzed include:

a) 20 shots used to study the 2-D cross-correlation functions (Zweben PoP '17)
b) 17 shots used to study the L-H transition (Diallo NF '17)
c) 140 shots used to study turbulence and blobs (Zweben NF '15 and Zweben PPCF '16)
d) 5 shots used to compare GPI with BES (Sechrest et al, PoP '15)
e) 27 shots used to characterize the effect of a deuterium gas puff (Zweben PPCF '14)
f) 4 shots used to compare GPI with DEGAS 2 (Cao et al, FST '13)

A list of the 140 shot database which was used for the 'scaling studies" in (c) can be found at: https://nstx.pppl.gov/nstx/Software/GPI/GPI_2010_Top_Shots.html and https://w3.pppl.gov/~szweben/NF2015/NF2015.html. These shots were chosen from the

322 shot list to have good GPI data during near-steady-state conditions within the analysis window of ±5 msec around the peak of the GPI gas puff (used to maximize the signal level), and to have no L-H transition and little or no MHD during this time (there are actually 150 shots there, 10 were later removed due to excessive MHD). Sample movies can be seen by clicking on the blue shot number.

A time sequence of GPI images from a typical shot in this data set is shown in Fig. 4, taken from Zweben et al, NF '15. For these images the raw camera data has been normalized to the time-averaged frame (over 1 msec) to remove the dependence of the signal on the GPI light emission profile, which is not relevant for the turbulence analysis. Normally the raw data signal peaks near the separatrix, where the Dα or HeI light emission is maximum. Details of the light emission process are described in Zweben et al, RSI '16 and Maqueda et al, RSI '03.

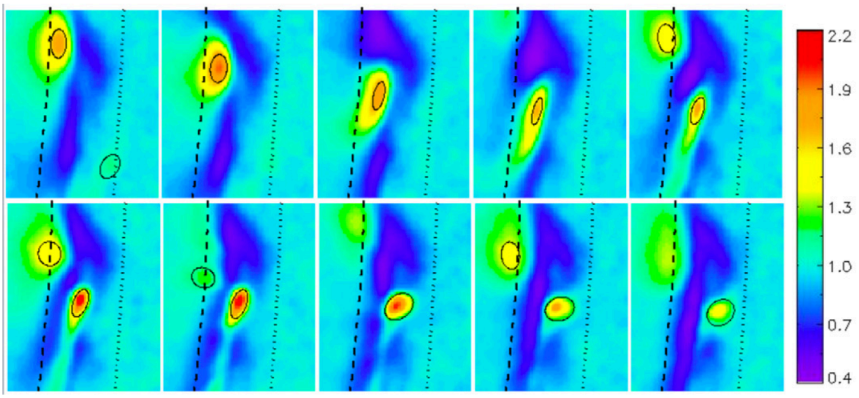

Figure 1. Sample images of the normalized GPI Dα light emission versus time for a typical H-mode shot during 4 MW of NBI (#140395). The time between these images is 10 μs (4 frames) and their size is ~30 cm poloidally (vertical) × 24 cm radial (horizontal). Each image is normalized to the time-averaged image, and the relative fluctuation levels are shown by the colour scale on the right. The location of blobs (defined in the text) is shown by the elliptical regions. The magnetic separatrix is the dashed line and the shadow of the limiter (RF antenna) is the dotted line (an online movie is linked here) (stacks.iop.org/NF/55/093035/mmedia).

Fig. 4 – time sequence of GPI images (showing every 4th frame of data)

4) Viewing and restoring GPI data

The simplest way to view the GPI data is to use the generic NSTX camera code "fcplayer" written by Bill Davis (Bill is retired and this code may not be working forever). To view GPI camera data for shot 141745: IDL> fcplayer, 141745, cam=5. This produces a widget which can be used to play the movies on the screen. There are many options under "file" and "edit" and "special" menus, including the normalization, blob tracking, and movie making ("file: write an animation file). A description of this code is given in Davis et al, FED '14 and Davis et al, PPPL-4877 (2013). This code works only for the 2010 Phantom 710 data.

To restore and view the data within IDL, the simplest code is:

```
IDL> /p/gpi/szweben/.r gpi_restore
IDL> gpi, shot=141741, tstart=210, tend=211, sm=1, nframes=40
```

This restores the GPI data from t=210 to 211 msec, smooths the data is 2d space by "sm" pixels, plays the unnormalized movie starting from 210 msec for 40 frames, then plots the average frame over this time, and then plays the normalized data for 40 frames. The output is re-binned from 64x80 to 128x240, the separatrix (dashed line), RF antenna (dotted line) and gas manifold position are overlaid as shown in Fig. 5. This code only works for the 2010 Phantom 710 data.

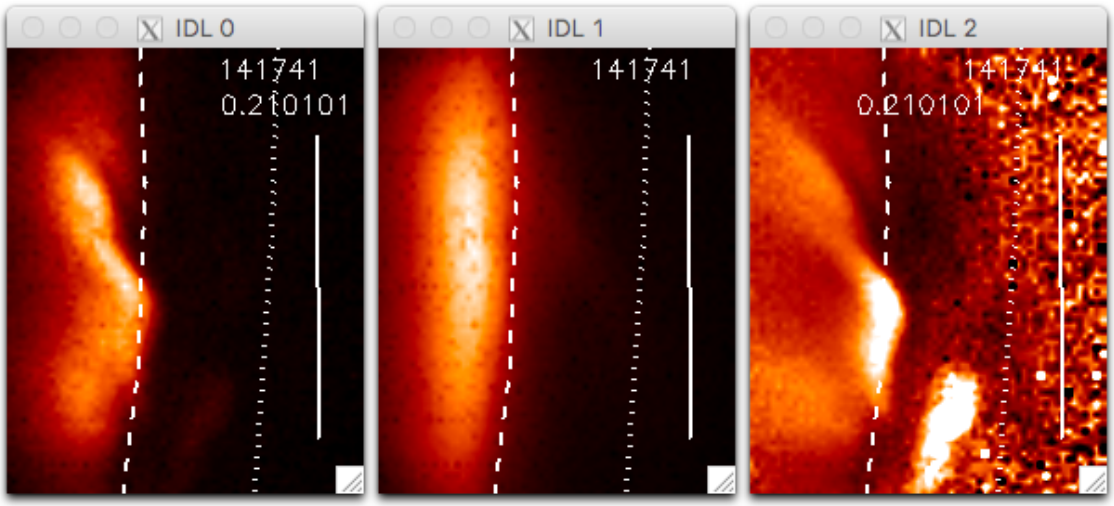

Fig. 5 - typical output of GPI_restore.pro

There are many GPI data analysis codes based on this restoration process, all of which are in the GPI project area: /p/gpi/szweben. A summary of the 2010 database including sample movies and a shot list can be found at: http://w3.pppl.gov/~szweben/NSTX2013/NSTX2013.html. Bill Davis' blob tracking code is described in: http://nstx.pppl.gov/nstx/Software/Applications/BlobTracking.html.

5. Data analysis issues for GPI

All of the known generic issues for GPI data analysis and interpretation were discussed in the GPI diagnostic review Zweben et al, RSI '17. Therefore in this section we focus on NSTX-specific issues.

a) separatrix location: the separatrix location within the GPI field of view was taken from the equilibrium code EFIT02 (which was run for nearly all shots), and translated into the GPI coordinates for the 2010 run using Ricky's calibration grid (rzmap.dat) and a code "oplotsep" written by Bill Davis (see gpi_restore.pro of Sec. 3). The uncertainty in the radial location of the outer midplane separatrix is ~1-2 cm, according to Steve Sabbagh (author of EFIT02). However, an alternative code equilibrium code LRDFIT is also available (as used for example in Boedo et al, PoP 21, 042309, 2014 and Agostini et al PoP '07). As far as we know, there has not been a systematic comparison between

these two codes, and so the separatrix location remains an open issue to some extent. This does not affect the GPI data directly, but does affect its interpretation when the separatrix location is important.

b) localization: the 2-D turbulence structure is imaged perfectly only when the GPI light emission is localized in a plane perpendicular to the local B field. This localization is compromised due to the finite extent of the GPI gas cloud along B and by a misalignment of the local B field with the local viewing direction. These issues were discussed extensively for NSTX data in Zweben et al, PoP '17, and shown to be relatively minor concerns at least near the center of the image plane for most shots. However, there are certainly cases in which the 3-D structure of the turbulence filaments is visible in the images, as also discussed in that paper. As a rough guide to identify these cases, the B field misalignment angle should be $\leq 10^{o}$ and the ratio of light emission with/without the gas puff should be ≥ 10. If the 3-D filamentary structure of the turbulence is visible in the images, caution should be used in interpreting the local turbulence properties. No attempt has been made to unfold the 2-D structure from such images in NSTX, but this has been attempted with passive imaging at MAST, Torpex, and Alcator C-Mod.

c) gas puff perturbations: for all the GPI analysis of edge turbulence on NSTX so far it has been assumed that the GPI gas puff does not significantly perturb the local plasma conditions or the local turbulence. This issue has been extensively discussed for NSTX deuterium data in the paper Zweben et al PPCF '14, in which some exceptions this assumption are also described. The deuterium gas puff does seem to cool and densify the edge in some shots, but only well after the peak of the GPI light signal ~20 msec after the start of gas injection. This was true for normal gas puffs of $\leq$ 5 Torr-liters with the specific gas injection system of NSTX; there will likely be more perturbation for larger and/or more localized puffs in other systems. All of the 322 shots in the 2010 GPI database were done using deuterium puffs, although some earlier GPI data was also taken with helium puffs in HeI light, e.g. in Zweben et al NF '04. There was very likely a larger edge perturbation with helium puffs, which led to the almost exclusive use of deuterium puffs in later runs; however, no explicit study was made of the helium puff perturbation in NSTX. In 2010 and 2016 there was an effect of the GPI puff on the CHERS background signal, which prevented use of CHERS and GPI at the same time (according to Ron Bell). This should be discussed in detail well before the next run.

d) shadowing: early simulations of GPI showed that that the turbulence itself can affect the neutral density profile and so affect the GPI light emission, a process known as "shadowing" (Stotler et al JNM '03). A similar shadowing process occurs with NBI in BES, as described in the GPI diagnostic review (Zweben et al RSI '17 and references therein). This process will tend to create a negative shadow radially inside a positive blob (and *vice versa*) due to the varying ionization of the neutral gas by the turbulence. Although there is no doubt that this process will occur to some extent, no clear evidence for shadowing has yet been seen in NSTX GPI data. In particular, the 2-D spatial cross-correlation study in Zweben et al PoP '17 showed no consistent pattern of negative cross-correlation which could be attributed to shadowing. A recent study of blob-hole pairs in NSTX (Myra et al PoP '18) showed that the minima in normalized GPI signals move

inward while the maxima move outward, in contrast to the expected shadowing effect. A simulation of the GPI shadowing effect in XGC1 simulations of Alcator C-Mod is underway (Stotler et al, JNM 2018).

e) turbulence velocity and flows: an important type of analysis for GPI data is to infer the poloidal and radial velocity of the turbulence, especially for use in comparing with theory. For example, the turbulence velocity for NSTX GPI was most recently analyzed in Diallo et al NF '17 to help understand the L-H transition. These analyses are based on various types of velocimetry, all of which have significant limitations and uncertainties which are difficult to quantify, and further analysis of NSTX velocimetry is in progress (Stoltfus-Dueck, 2018). The relationship between the inferred turbulence velocity and the local fluid flow velocity is not entirely clear, since perturbations like drift waves can propagate in a fluid at rest. Thus radial transport has not (yet) been inferred from NSTX GPI data, since the radial fluid velocity is needed, along with the density and/or temperature fluctuations, which are also not directly measured by GPI.

f) MHD effects: the effects of strong MHD activity in the edge can be seen in GPI as long-poloidal wavelength radial or amplitude modulation of the GPI light emission, but for most shots these effects are not visible. Some examples from 2004 can be seen at: https://w3.pppl.gov/~szweben/Othervideo/NSTX04/NSTX_04.html. The NSTX GPI data has been explicitly used to study ELMS (Maqueda et al PoP '09, JNM '09 and Sechrest et al NF '12), but has not (yet) been used to study other MHD modes. A quasi-coherent drift-wave like mode has also been seen in Ohmic GPI data in NSTX (Banerjee PoP '16), and in Alcator C-Mod, e.g. Theiler et al, PPCF 59, 025016 (2017). In general, we assume that the effects of MHD are to modulate the edge plasma parameters and/or separatrix position, and that the edge turbulence physics is independent of the large-scale MHD modes due to the differing size scales.

g) RF effects: many discharges in NSTX have RF heating, but so far no explicit account has been taken of the effect of RF waves on the interpretation of GPI data. It is possible that strong RF heating could cause significant non-Maxwellian ions and/or electrons in the edge and SOL, and this might affect the dependence of the GPI line emission on the local temperature and density. However, no signs of any unusual effects have so far been seen in GPI data, which generally looks similar to NBI data (see https://w3.pppl.gov/~szweben/NSTX2013/NSTX2013.html.

h) synthetic GPI diagnostic: all analysis of GPI turbulence data has been done using the direct light emission data without any attempt to unfold the density or temperature fluctuations before the analysis (as described in Zweben et al RSI '17). However, when comparing this GPI data analysis to theory, a "synthetic GPI diagnostic" is often applied to the calculated density and temperature fluctuations to convert them into GPI line emission fluctuations, for example in Russell et al PoP '11. However, the inferred turbulence quantities such as the correlation lengths and turbulence velocities are normally not significantly changed by this process. A more ambitious synthetic diagnostic can include a calculation of the neutral density profile using a code like

DEGAS 2, as in Cao et al FST '13. A detailed synthetic GPI diagnostic for XGC1 runs for NSTX has been started but not yet completed (Stotler, 2018).

6. Possible GPI hardware upgrades for NSTX-U

This section outlines some potential GPI hardware upgrades which could be done before or after the re-start of NSTX-U.

a) add 2nd Phantom 710 for "side view" of GPI gas cloud from the across the machine
- preliminary design and planning was done by Filippo Scotti in 2017)
- use 2nd PPPL Phantom 710 now at GA (P28620 now owned by Raffi Nazikian)
- measure average parallel length of gas cloud to determine GPI spatial resolution
- synchronize frames with main GPI camera to view individual filaments in 3d
- develop diagnostic to measure edge magnetic field line angle inside cloud
- further validate DEGAS 2 and XGC1 neutral physics using 3d cloud images

b) add remote control of ex-vessel re-entrant GPI optics inside Bay B midplane port
- some thinking about this was done by Gus Smalley and Stewart in 2016
- 2010 GPI results had loss of resolution in shots at largest B field misalignments
- 2016 optics has a manual adjustment of zoom and pan, not very useful for a run
- search for sub-cm structure needs shot-to-shot zoom/pan to align view with B
- suitable remote control can be designed by Gus Smalley (but needs some time)
- ideally this system should be spatially calibrated during a vessel opening

c) improved GPI gas injector (present 30 hole gas manifold has been used since 2002)
- some thinking about this was done by Stewart in 2017
- present gas injector is un-collimated, with ~10-15 cm GPI cloud length along B
- TEXTOR developed simple collimated GPI injector (Shesterikov RSI '13)
- new design should be tested and calibrated using off-line vacuum chamber
- can replace present manifold with collimated design, or add it nearby
- could also investigate controlled dust injector, e.g. for seeding blobs

d) add C-Mod GPI avalanche photodiode (APD) arrays to augment present GPI camera
- proposed for NSTX-U within MIT-PPPL collaboration by Jim Terry in 2013 (see folder "GPI future plans/APD installation by MIT" in GPI Guide)
- these detectors are more sensitive and faster than 710 camera, in 9x10 array
- can potentially extend GPI to ~1 MHz and/or farther inward radially
- work needed to install new optics and electronics in basement is identified
- this upgrade can be done without any in-vessel activity, with post-calibration

e) add "thermal helium beam" (THB) to existing GPI view (i.e. for helium line ratios)
- proposed collaboration for NSTX-U by RFX (Padova) group in 2015 (see folder "GPI future plans/helium line ratio" in GPI Guide)
- can measure edge electron density and temperature fluctuations (and profiles)
- not sure if Padova hardware is still available, but other hardware options exist

- requires significant interface work, e.g. fiber penetrations and new rack
- good theory/modeling work for NSTX-U done by Muñoz Burgos (PoP 2016)

f) new GPI view(s) to measure 3d turbulence structure
- proposed by T. Munsat in 2012 (see "GPI future plans/3D view" in GPI Guide)
- easiest way is backward view along B from existing port to edge of RF limiter
- new GPI gas sources can be installed using narrow capillary tubes
- also relatively easy is new radial view of center column gas puffer
- divertor plate GPI would be useful to correlate with divertor Langmuir probes

g) new GPI camera for much higher speed/sensitivity can be purchased for ~$100k
- LLNL recently bought a Phantom v1211 with 5x higher sensitivity than v710
- Photron FASTCAM SA-Z from Japan may be competitive.

7) Further GPI analysis with existing data

There is a lot of further analysis which can be done with existing NSTX GPI data (mainly from 2010, 2009). Examples are:

a) blob creation and shape evolution

The spatial structure and motion of blobs in NSTX was studied using Bill Davis' blob tracking code based on a 14 shot subset of the 2010 database (Zweben et al 2016). However, this code defined a "blob" using an arbitrary selection criterion and fit the detected blobs with an ellipse, so it did not attempt to determine how blobs formed, split, or merged. A separate study was done on the relationship of local shear flow to blob dynamics using a Reynolds stress proxy (Myra et al 2013), but with the same definition of the blob shape. Thus further analysis could be done to better define how blobs are formed, how their shapes evolve, and even how blobs interact with each other. It would be particularly interesting to compare these results with analytic blob theory and/or edge turbulence simulations such as XGC1 or SOLT. The results could be important for understanding the part of the SOL width due to blobby transport.

b) continued search for the mechanism of L-H transition

The L-H transition as seen in NSTX GPI was studied using 17 shots in the 2010 database (Diallo et al, NF '17), and previously studied a few L-H transitions from the 2009 database (Zweben et al, POP '10). Yet it is still not clear what causes the L-H transition in NSTX (or other machines). There are probably not many more good L-H transition shots in these GPI databases, but another search for them could be done, and the analysis of the 2017 paper could be redone using improved 2-D structure analysis and velocimetry to look for subtle changes before the transition. Recent L-H transition theories and simulations should be consulted for clues as to what to look for. Evidence from other diagnostics (BES, reflectometer, high-k, edge USXR, MHD, other cameras) may be useful to add to the picture. Back-transitions in GPI have not yet been studied, but probably should be (these are sometimes complicated by ELM events).

c) cross-comparisons of GPI with BES, probe, reflectometer, high-k fluctuation data

A detailed comparison of GPI and BES results was done by Sechrest and Smith (PoP '15), with fairly good agreement except for the relative fluctuation level, which was nearly 10x larger in GPI than BES. This should be revisited and resolved. Rough agreement was found between the UCSD Langmuir probe results and GPI results (Boedo et al, Phys. Plasmas 21, 042309 (2014), but not by direct comparison within a single shot. Four common shots were found in the 2010 run in 2017 (142275, 142234, 142232, 142230), and some analysis was done on that GPI data (see "Comparison of GPI with probe" in GPI shot lists folder in Guide), but the probe analysis was never finished. Direct comparison with the UCLA reflectometer data should be possible, and was started in collaboration with S. Kubota about 2013-4, but was never finished. Comparison with high-k scattering might be interesting, but was never done since the high-k system of 2010 apparently did not have overlapping (edge) channels.

d) look for effects in GPI of RMP, divertor shape, RF power

It is possible that variations in the applied RMP fields (especially with divertor footprint splitting), or the shape of the edge magnetic surfaces (e.g. snowflake divertors), or the applied RF (especially when coupled to edge heating) can affect edge turbulence, but their effects in NSTX GPI have not been obvious and so have not yet been studied in detail. But there was relatively little systematic variation of the GPI results even with a large variation in NBI power 0-6 MW (Zweben NF '15). The first step would be to cross-check the 2010 GPI shot list for systematic variations in these parameters over a narrow range of current and field, and create shot lists. Then the GPI movies for various cases should be viewed to see the overall turbulence picture. Then standard turbulence quantities (correlation lengths and time, fluctuation level, turbulence velocities) should be plotted vs. the variable of interest. Of course, it may be difficult to isolate the effect of interest due to co-variations with other quantities, e.g. edge density, so it would help to have some ideas from theory to know what to look for.

e) search for neutral 'shadowing' effects in GPI data

This was already discussed in 4(d). New data analysis could be done to look for shadowing due to very large blobs, perhaps by conditional sampling. Calculations should be done of the expected effects for NSTX GPI conditions (i.e. the amount of ionization in large blobs compared with the gas influx), perhaps with DEGAS 2. Recent theory should be consulted for ideas about what to look for (see Zweben RSI '17 and Stotler JNM '18 for references). Perhaps the theorists who have calculated GPI shadowing (e.g. Wersal and Ricci, NF '17) might be interested in collaborating on this analysis.

f) analyze 2016 "passive" data taken with GPI view (without gas puffing)

There is a list of ~100 shots in the GPI Guide folder "shot lists", and Filippo has already used this data to study cross-correlations with NSTX passive divertor imaging (Scotti PPCF '18) and for evaluating the neutral density. However, it is hard to determine the turbulence characteristics from this data due to the limited framing rate (100 kHz) and the lack of localization. It might be interesting to measure the B field line direction from the 3D turbulence filament orientations in this view (assuming the filaments lie along B field lines), and compare the results with EFIT or LRDFIT.

g) transport effects from GPI

No direct inference of edge or SOL transport has been made from NSTX GPI data, although this may be possible and if so would be very interesting. Some of the difficulties in this process were described for C-Mod GPI data in Zweben, Terry et al, J. Nucl. Mat. 415, S463 (2011), and theory-based scalings were discussed in Myra PoP '16. Radial particle or heat transport estimates require a radial velocity, which can come from GPI velocimetry measurements, and local density and/or temperature fluctuations, which could come from a theoretical model of the GPI light emission (e.g. assuming a relative density to temperature fluctuation level). This can be done separately for broadband turbulence and for discrete blobs. The results will probably be quite uncertain, but it might be useful to look for trends, e.g. with the divertor heat flux SOL width or divertor plate light emission profile.

h) validation of edge turbulence simulations (SOLT, XGC1, BOUT, GBS)

The most detailed comparisons of GPI data with edge turbulence simulations were done for the 2D turbulence code SOLT, e.g. Myra PoP '16 and Russell PoP '15. There were many similarities but also some differences between this code and the GPI data, which could certainly be analyzed further. We are still awaiting an XGC1 run for NSTX, but a comparison of C-Mod GPI with XGC1 has started (R. Churchill and D. Stotler, 2018). BOUT++ is being run for MAST (Militello et al, PPCF '16), and could be run for NSTX if someone was interested. The Lausanne code GBS was run to compare with inner-wall limited C-Mod GPI data (Halpern PoP 24, 072502 (2017)), but Halpern has moved to GA and is doing different work now.

8. Future experiments on NSTX-U

a) correlate GPI data with divertor plate heat/particle SOL widths

Up to now there has been no direct attempt to correlate NSTX GPI turbulence results with the heat/particle SOL widths measured at the NSTX divertor plate, although some connection was attempted for edge harmonic oscillation (EHO) discharges by Gan et al, Nucl. Fus. 57, 126053 (2017). Qualitatively, one expects that the SOL widths should increase with increased edge turbulence fluctuation level, radial correlation length, and/or radial velocity, although the transport is difficult to quantify from GPI data (see Sec. 7(g)). An XP was planned for the 2016 run to pursue this topic, in collaboration with T. Gray and XGC1 modeling by C.S. Chang (OP-XP-1514, "Relationship Between Plasma Turbulence and SOL Width Scaling in NSTX-U", see GPI Guide in folder "GPI future plans/XPs") – but this was never started due to the outage. Measurements could be made with GPI at the same time as the IR divertor camera divertor (Gray), visible divertor cameras (Scotti), divertor Langmuir probes (Jaworksi), and all other edge/SOL fluctuation and plasma diagnostics (BES, reflectometry, high-k scattering, CHERS, etc). Special attention should be given to L-H transitions (which shows the largest systematic variations in GPI edge turbulence), current scans (which show the largest variation in SOL heat flux width), and NBI and RF power scans (which show the largest variations in power loss). Careful thought should be given to isolating and identifying possible ion neoclassical losses, which might be significant in NSTX (especially at low current).

b) search for small-scale (e.g. ETG) turbulence with GPI zoom and q(a) scan

The zoom lens GPI hardware upgrade was done in 2015 by graduate student Noah Mandell and Gus Smalley, and was designed to look for small-scale structure in the existing GPI view (see GPI guide folder "GPI zoom optics"). At maximum zoom the optical spatial resolution of this system is ~1 mm at the GPI target plane, which is about x5 better than the 2010 system. However, for this to be useful in resolving small-scale turbulence, the alignment of the local B field line must be close to the optical alignment; thus a q(a) scan was built into the Noah's XP planned for 2016. But the zoom feature was never used for the 2016 run due to the outage, and all the "passive" 2016 GPI data was taken at nearly the same wide field field of view as for the 2010 run. The zoom lenses caused strong vignetting which is not optimal for the wide view, and so a decision should be made well before the next run whether to keep the zoom lenses to search for small-scale structure, or go back to normal lenses to use with the previous field of view. If zoom lenses are used, they should be supplemented with remotely controlled pan/tilt, as described in Sec. 5(b).

c) measure edge q(r) using edge turbulence filaments

Filippo is already planning a 2nd fast camera view of the GPI gas puff from the other side of NSTX-U, as described in Sec. 5(a). With this and the usual GPI camera running at the same time, the filamentary structures should be visible in both the radial vs. poloidal and poloidal vs. toroidal views. If the individual filaments can be identified in both views on the few-μsec timescale (a non-trivial task), it should be possible to determine the filament location and angular orientation in 3D and compare it with the B field line angle from EFIT or LRDFIT. This is interesting especially when the edge bootstrap current is large, or when heating or current drive is expected to change the edge current profile. Note that the edge filaments might have a small but finite angle perpendicular to B if they have a drift-wave structure, but they should be aligned with B in the SOL if they have a simple interchange structure. This would also be interesting to check.

d) measuring edge density and temperature fluctuations

Matteo Agostini and Paolo Scarin proposed in 2015 to bring the RFX helium line ratio diagnostic to NSTX for use with the GPI view, but this was never done due to the outage (see folder in GPI Guide "GPI future plans/Helium line ratio"). This could in principle measure separately both the electron density and temperature fluctuations, as discussed in the papers by Burgos there. Although this is a difficult diagnostic due to the limited light emission and the possible perturbing effect of helium puffing in NSTX-U, the results would be very useful for physics understanding of the edge turbulence. Some information might also come from by simply puffing both deuterium and helium together and comparing the fluctuations in the two species' lines with two cameras, since these lines have different dependences on density and temperature. Oliver Schmitz was also interested in this diagnostic in 2016 and discussed a collaboration with NSTX-U.

d) understanding lithium conditioning

There is little if any understanding of why lithium wall coating affects the plasmas in NSTX. Bin Cao looked for changes in GPI with lithium conditioning (Cao

PPCF ’12), but saw only slight increases of poloidal turbulence velocity with increased lithium. Dave Russell studied the effect of pedestal profile changes due to lithium on edge turbulence as seen in SOLT modeling (Russell PoP ’15). Some decrease in the relative fluctuation levels in GPI data was seen in the 2010 database (Zweben NF ’15), but at least some of this was due to the prevalence of H-modes with increased lithium. It would be worthwhile to revisit the search for correlations between lithium coating and the edge turbulence seen in GPI. Such correlation might be due to the presence of lithium ions directly (e.g. due the parallel resonances with the turbulence), or indirectly due to systematic changes in the edge plasma profiles with lithium, as in R. Maingi et al, NF 52, 083001 (2012).

e) effects of neutrals/impurity injection on GPI

The effects of the GPI deuterium puff on the edge plasma of NSTX in the 2010 GPI database was studied in Zweben et al, PPCF ’15, but relatively little effect on the plasma was seen at least up to ~50 msec after the peak of the puff. At later time this puff sometimes cooled the plasma, but did not significantly change the edge turbulence as seen by GPI. This study should be extended to include a wider range of deuterium puff strengths and also impurity puffing, especially to determine the effect of helium GPI puffing on the edge plasma. It would also be interesting to puff neon, argon, or methane, to see the filamentary structure in the ion lines and the effects of these local perturbations on the edge turbulence. This was done a little bit in early in NSTX, but the light level was not enough (or the puff levels were not large enough) to see the turbulence clearly. It might also be interesting to look at injected dust or pellets.

9. Possible future collaborations on GPI

a) Ralph Kube (Tromso) – is preparing a proposal for the Norwegian Research Council on “Transport statistics of turbulent plasma flows”, including data from NSTX and C-Mod GPI systems. Stewart will try to collaborate on this after retirement.

b) Jim Myra and other Lodestar people will probably continue to collaborate with Filippo on divertor filaments and edge turbulence in NSTX-U

c) Santanu Banerjee (IPP India) will continue to collaborate with Ahmed and Tim on velocimetry and L-H transitions in NSTX

d) Jim Terry and other MIT people might want to restart the collaboration planned for NSTX-U, based on the C-Mod APD array

e) an attempt was made to collaborate with on a MAST GPI system (with J. Harrison and S. Mordijk), but this was never finalized; this might be revived

f) other possible GPI collabrations with RFX, DIII-D, EAST, W7-X, TCV, AUG, HL-2A, India - see GPI review: RSI 88, 041101 (2017) for list of GPI systems.

10. List of publications (list from Web of Science)

sorted as "Experimental", "Diagnostic and Hardware" and "Theory and Modeling"
most of the relevant papers and talks/posters are at:

http://w3.pppl.gov/~szweben/Papers/szpaperslist.html
http://w3.pppl.gov/~szweben/Talks/talks.html

Experimental results:

Two-dimensional turbulence cross-correlation functions in the edge of NSTX
By: Zweben, S. J.; Stotler, D. P.; Scotti, F.; et al.
PHYSICS OF PLASMAS Volume: 24 Issue: 10 Article Number: 102509 Published: OCT 2017

Energy exchange dynamics across L-H transitions in NSTX
By: Diallo, A.; Banerjee, S.; Zweben, S. J.; et al.
NUCLEAR FUSION Volume: 57 Issue: 6 Article Number: 066050 Published: JUN 2017

Observation of quasi-coherent edge fluctuations in Ohmic plasmas on National Spherical Torus Experiment
By: Banerjee, Santanu; Diallo, A.; Zweben, S. J.
PHYSICS OF PLASMAS Volume: 23 Issue: 4 Article Number: 044502 Published: APR 2016

Blob structure and motion in the edge and SOL of NSTX
By: Zweben, S. J.; Myra, J. R.; Davis, W. M.; et al.
Group Author(s): NSTX-U Team
PLASMA PHYSICS AND CONTROLLED FUSION Volume: 58 Issue: 4 Article Number: 044007 Published: APR 2016

Edge and SOL turbulence and blob variations over a large database in NSTX
By: Zweben, S. J.; Davis, W. M.; Kaye, S. M.; et al.
Group Author(s): NSTX Team
NUCLEAR FUSION Volume: 55 Issue: 9 Article Number: 093035 Published: SEP 2015

Comparison of beam emission spectroscopy and gas puff imaging edge fluctuation measurements in National Spherical Torus Experiment
By: Sechrest, Y.; Smith, D.; Stotler, D. P.; et al.
PHYSICS OF PLASMAS Volume: 22 Issue: 5 Article Number: 052310 Published: MAY 2015

Effect of a deuterium gas puff on the edge plasma in NSTX
By: Zweben, S. J.; Stotler, D. P.; Bell, R. E.; et al.
PLASMA PHYSICS AND CONTROLLED FUSION Volume: 56 Issue: 9 Article Number: 095010 Published: SEP 2014

COMPARISON OF GAS PUFF IMAGING DATA IN NSTX WITH DEGAS 2 SIMULATIONS

By: Cao, B.; Stotler, D. P.; Zweben, S. J.; et al.
FUSION SCIENCE AND TECHNOLOGY Volume: 64 Issue: 1 Pages: 29-38 Published: JUL 2013

Two-dimensional characterization of ELM precursors in NSTX
By: Sechrest, Y.; Munsat, T.; Battaglia, D. J.; et al.
NUCLEAR FUSION Volume: 52 Issue: 12 Article Number: 123009 Published: DEC 2012

Edge turbulence velocity changes with lithium coating on NSTX
By: Cao, B.; Zweben, S. J.; Stotler, D. P.; et al.
PLASMA PHYSICS AND CONTROLLED FUSION Volume: 54 Issue: 11 Article Number: 112001 Published: NOV 2012

Intermittency in the scrape-off layer of the National Spherical Torus Experiment during H-mode confinement
By: Maqueda, R. J.; Stotler, D. P.; Zweben, S. J.
Group Author(s): NSTX Team
Conference: 19th International Conference on Plasma-Surface Interactions in Controlled Fusion Devices (PSI) Location: Univ Calif, Gen Atom, San Diego, CA Date: MAY 24-28, 2010 Sponsor(s): Lawrence Livermore Natl Lab
JOURNAL OF NUCLEAR MATERIALS Volume: 415 Issue: 1 Supplement: S Pages: S459-S462 Published: AUG 1

Flow and shear behavior in the edge and scrape-off layer of L-mode plasmas in National Spherical Torus Experiment
By: Sechrest, Y.; Munsat, T.; D'Ippolito, D. A.; et al.
PHYSICS OF PLASMAS Volume: 18 Issue: 1 Article Number: 012502 Published: JAN 2011

Quiet periods in edge turbulence preceding the L-H transition in the National Spherical Torus Experiment
By: Zweben, S. J.; Maqueda, R. J.; Hager, R.; et al.
PHYSICS OF PLASMAS Volume: 17 Issue: 10 Article Number: 102502 Published: OCT 2010

Intermittent divertor filaments in the National Spherical Torus Experiment and their relation to midplane blobs
By: Maqueda, R. J.; Stotler, D. P.
Group Author(s): NSTX Team
NUCLEAR FUSION Volume: 50 Issue: 7 Article Number: 075002 Published: JUL 2010

Secondary ELM filaments in NSTX
By: Maqueda, R. J.; Maingi, R.; Ahn, J. -W.
Group Author(s): NSTX Team
Conference: 18th International Conference on Plasma-Surface Interactions in Controlled Fusion Devices Location: Toledo, SPAIN Date: MAY 26-30, 2008
Sponsor(s): Spanish Natl Fus Lab; Spanish Minist Sci & Innovat
JOURNAL OF NUCLEAR MATERIALS Volume: 390-91 Pages: 843-846 Published: JUN 15 2009

Primary edge localized mode filament structure in the National Spherical Torus Experiment
By: Maqueda, R. J.; Maingi, R.
Group Author(s): NSTX team,
Conference: 50th Annual Meeting of the Division of Plasma Physics of the American-Physical-Society Location: Dallas, TX Date: FEB 01, 2008
Sponsor(s): Amer Phys Soc, Div Plasma Phys
PHYSICS OF PLASMAS Volume: 16 Issue: 5 Article Number: 056117 Published: MAY 2009

Study of statistical properties of edge turbulence in the National Spherical Torus Experiment with the gas puff imaging diagnostic
By: Agostini, M.; Zweben, S. J.; Cavazzana, R.; et al.
PHYSICS OF PLASMAS Volume: 14 Issue: 10 Article Number: 102305 Published: OCT 2007

Impact of different confinement regimes on the two-dimensional structure of edge turbulence
By: Alonso, J. A.; Zweben, S. J.; Carvalho, P.; et al.
Group Author(s): TH-II Team
Conference: 33rd European-Physical-Society Conference on Plasma Physics Location: Angelicum Univ, Rome, ITALYDate: JUN 19-23, 2006
Sponsor(s): Assoc EURATOM-ENEA Fusione; European Phys Soc
PLASMA PHYSICS AND CONTROLLED FUSION Volume: 48 Issue: 12B Special Issue: SI Pages: B465-B473 Published: DEC 2006

Bispectral analysis of low- to high-confinement mode transitions in the National Spherical Torus Experiment
By: White, A. E.; Zweben, S. J.; Burin, M. J.; et al.
PHYSICS OF PLASMAS Volume: 13 Issue: 7 Article Number: 072301 Published: JUL 2006

Derivation of time-dependent two-dimensional velocity field maps for plasma turbulence studies
By: Munsat, T.; Zweben, S. J.
REVIEW OF SCIENTIFIC INSTRUMENTS Volume: 77 Issue: 10 Article Number: 103501 Published: OCT 2006

Structure and motion of edge turbulence in the national spherical torus experiment and alcator C-mod
By: Zweben, S. J.; Maqueda, R. J.; Terry, J. L.; et al.
Conference: 47th Annual Meeting of the Division of Plasma Physics of the American-Physical-Society Location: Denver, CO Date: OCT 24-28, 2005
Sponsor(s): Amer Phys Soc, Div Plasma Phys
PHYSICS OF PLASMAS Volume: 13 Issue: 5 Article Number: 056114 Published: MAY 2006

Images of edge turbulence in NSTX
By: Zweben, SJ; Bush, CE; Maqueda, RJ; et al.

IEEE TRANSACTIONS ON PLASMA SCIENCE Volume: 33 Issue: 2 Pages: 446-447 Part: 1 Published: APR 2005

High-speed imaging of edge turbulence in NSTX
By: Zweben, SJ; Maqueda, RJ; Stotler, DP; et al.
Group Author(s): NSTX Team
NUCLEAR FUSION Volume: 44 Issue: 1 Pages: 134-153 Article Number: PII S0029-5515(04)71999-7 Published: JAN 2004

Diagnostics and Hardware:

Invited Review Article: Gas puff imaging diagnostics of edge plasma turbulence in magnetic fusion devices
By: Zweben, S. J.; Terry, J. L.; Stotler, D. P.; et al.
REVIEW OF SCIENTIFIC INSTRUMENTS Volume: 88 Issue: 4 Article Number: 041101 Published: APR 2017

Fast 2-D camera control, data acquisition, and database techniques for edge studies on NSTX
By: Davis, W. M.; Ko, M. K.; Maqueda, R. J.; et al.
Conference: 9th IAEA Technical Meeting on Control, Data Acquisition and Remote Participation for Fusion ResearchLocation: Hefei, PEOPLES R CHINA Date: MAY 06-10, 2013
FUSION ENGINEERING AND DESIGN Volume: 89 Issue: 5 Pages: 717-720 Published: MAY 2014

Advances in fast 2D camera data handling and analysis on NSTX
By: Davis, W. M.; Patel, R. I.; Boeglin, W. U.; et al.
Conference: 7th IAEA Technical Meeting on Control, Data Acquisition and Remote Participation for Fusion ResearchLocation: Aix-en-Provence, FRANCE Date: MAY 15-JUN 19, 2009
Sponsor(s): IAEA; French Commissariat Energie Atom, Inst Res Magnet Fusion
FUSION ENGINEERING AND DESIGN Volume: 85 Issue: 3-4 Pages: 325-327 Published: JUL 2010

Storage and analysis techniques for fast 2D camera data on NSTX
By: Davis, W. M.; Mastrovito, D. M.; Bush, C. E.; et al.
Conference: 5th IAEA Technical Meeting on Control, Data Acquisition, and Remote Participation for Fusion ResearchLocation: Budapest, HUNGARY Date: JUL 12-15, 2005
Sponsor(s): IAEA
FUSION ENGINEERING AND DESIGN Volume: 81 Issue: 15-17 Special Issue: SI Pages: 1975-1979 Published: JUL 2006

Gas puff imaging of edge turbulence (invited)
By: Maqueda, RJ; Wurden, GA; Stotler, DP; et al.
Conference: 14th Topical Conference on High-Temperature Plasma Diagnostics Location: MADISON, WISCONSIN Date: JUL 08-11, 2002
Sponsor(s): Univ Wisconsin Madison; Amer Phys Soc, Div Plasma Phys; US DOE, Off Fus Energy Sci & Defense Sci

REVIEW OF SCIENTIFIC INSTRUMENTS Volume: 74 Issue: 3 Special Issue: SI Pages: 2020-2026 Part: 2 Published: MAR 2003

Edge turbulence measurements in NSTX by gas puff imaging
By: Maqueda, RJ; Wurden, GA; Zweben, S; et al.
Conference: 13th Topical Conference on High-Temperature Plasma diagnostics Location: TUCSON, ARIZONA Date: JUN 18-22, 2000
Sponsor(s): Los Alamos Natl Lab, Phys Div; Los Alamos Natl Lab, Inertial Confinement Fus & Radiat Phys Program; Gen Atom; Amer Phys Soc, Div Plasma Phys; US DOE, Off Fus Energy Sci; US DOE, Off Def Sci
REVIEW OF SCIENTIFIC INSTRUMENTS Volume: 72 Issue: 1 Pages: 931-934 Part: 2 Published: JAN 2001

Theory and Modeling

Blob-hole correlation model for edge turbulence and comparisons with NSTX GPI data
J.R. Myra, S.J. Zweben, D.R. Russell, submitted to Phys. Plasmas (2018)

Theory based scaling of edge turbulence and implications for the scrape-off layer width
By: Myra, J. R.; Russell, D. A.; Zweben, S. J.
PHYSICS OF PLASMAS Volume: 23 Issue: 11 Article Number: 112502 Published: NOV 2016

Modeling the effect of lithium-induced pedestal profiles on scrape-off-layer turbulence and the heat flux width
By: Russell, D. A.; D'Ippolito, D. A.; Myra, J. R.; et al.
PHYSICS OF PLASMAS Volume: 22 Issue: 9 Article Number: 092311 Published: SEP 2015

Edge sheared flows and the dynamics of blob-filaments
By: Myra, J. R.; Davis, W. M.; D'Ippolito, D. A.; et al.
NUCLEAR FUSION Volume: 53 Issue: 7 Article Number: 073013 Published: JUL 2013

Diffusive-convective transition for scrape-off layer transport and the heat-flux width
By: Myra, J. R.; Russell, D. A.; D'Ippolito, D. A.
PLASMA PHYSICS AND CONTROLLED FUSION Volume: 54 Issue: 5 Article Number: 055008 Published: MAY 2012

Turbulent transport and the scrape-off-layer width
By: Myra, J. R.; Russell, D. A.; D'Ippolito, D. A.; et al.
Conference: 19th International Conference on Plasma-Surface Interactions in Controlled Fusion Devices (PSI) Location: Univ Calif, Gen Atom, San Diego, CA Date: MAY 24-28, 2010
Sponsor(s): Lawrence Livermore Natl Lab
JOURNAL OF NUCLEAR MATERIALS Volume: 415 Issue: 1 Supplement: S Pages: S605-S608 Published: AUG 1

Comparison of scrape-off layer turbulence simulations with experiments using a synthetic gas puff imaging diagnostic
By: Russell, D. A.; Myra, J. R.; D'Ippolito, D. A.; et al.
Group Author(s): NSTX Team
PHYSICS OF PLASMAS Volume: 18 Issue: 2 Article Number: 022306 Published: FEB 2011

Reduced model simulations of the scrape-off-layer heat-flux width and comparison with experiment
By: Myra, J. R.; Russell, D. A.; D'Ippolito, D. A.; et al.
Group Author(s): NSTX Team
PHYSICS OF PLASMAS Volume: 18 Issue: 1 Article Number: 012305 Published: JAN 2011

Saturation mechanisms for edge turbulence
By: Russell, D. A.; Myra, J. R.; D'Ippolito, D. A.
PHYSICS OF PLASMAS Volume: 16 Issue: 12 Article Number: 122304 Published: DEC 2009

Progress towards the validation of models of the behavior of neutral helium in gas puff imaging experiments
By: Stotler, D. P.; Boedo, J.; LeBlanc, B.; et al.
Conference: 17th International Conference on Plasma-Surface Interactions in Controlled Fusion Devices Location: Hefei, PEOPLES R CHINA Date: MAY 22-26, 2006
Sponsor(s): Inst Plasma Phys; Chinese Acad Sci, Bur Int Cooperat; Natl Nat Sci Fdn China
JOURNAL OF NUCLEAR MATERIALS Volume: 363 Pages: 686-692 Published: JUN 15 2007

Blob birth and transport in the tokamak edge plasma: Analysis of imaging data
By: Myra, J. R.; D'Ippolito, D. A.; Stotler, D. P.; et al.
PHYSICS OF PLASMAS Volume: 13 Issue: 9 Article Number: 092509 Published: SEP 2006

Three-dimensional neutral transport simulations of gas puff imaging experiments
By: Stotler, DP; D'Ippolito, DA; LeBlanc, B; et al.
Conference: 9th International Workshop on Plasma Edge Theory in Fusion Devices Location: Univ Calif, San Diego, San Diego, CA Date: SEP 03-05, 2003
Sponsor(s): UCSD, Engn Dept; Lawrence Livetmore Natl Lab; Off Fus Enegy, Dept Energy; Max-Planck Inst Plasma Phys
CONTRIBUTIONS TO PLASMA PHYSICS Volume: 44 Issue: 1-3 Pages: 294-300 Published: 2004